Development of confocal picosecond ultrasonics for visualizing propagation of acoustic wave

Nobutomo Nakamura [1*], Atsushi Maehara[1], and Hirotsugu Ogi [2]

[1] *Graduate School of Engineering Science, Osaka University, Toyonaka, Osaka 560-8531, Japan*
[2] *Graduate School of Engineering, Osaka University, Suita, Osaka 565-0871, Japan*

For visualizing propagation of acoustic wave and evaluating local sound velocity in micro/nano-meter structures, confocal picosecond ultrasonics is developed. In conventional picosecond ultrasonics, measurement of local sound velocity was difficult, and macroscopic sound velocity and elastic properties were measured. However, in the confocal picosecond ultrasonics, a confocal laser-scanning microscope is embedded in the optics of the picosecond ultrasonics, and depth resolution is improved. Using the developed optics, we successfully observed propagation of an acoustic wave in thin film. In this paper, the optics we developed and experimental results on silica film are reported.

Picosecond ultrasonics[1)] is a powerful method for exciting acoustic waves and for evaluating acoustical properties in micro/nano-meter structures, and it has been applied for several materials such as multilayers,[2–6)] glasses,[7–9)] piezoelectric materials,[10,11)] metallic films,[12–14)] and biological materials.[15–17)] In picosecond ultrasonics, sub-terahertz acoustic wave is generated and detected using the pump-probe technique, and sound velocity and attenuation averaged over the propagation path where the acoustic wave travels are measurable. However, visualization of propagation of the acoustic wave and evaluation of local properties are quite difficult using the picosecond ultrasonics, although three-dimensional imaging is performed using the wavelet transforms.[17)] In bulk materials, propagation of the acoustic wave is visualized using the photoelastic technique.[18)] By using the photoacoustic method[19)] and phased array sensors,[20)] three-dimensional structure inside a specimen can be visualized. However, it is difficult to apply these methods for small materials. In this study, for visualizing the propagation of acoustic waves in micro/nano-meter structures, the confocal picosecond ultrasonics is developed.

In optical microscopy, development of the confocal optics improved the resolution in the depth direction significantly,[21)] and the confocal microscopy is nowadays used widely.[22–24)]

*E-mail: nobutomo@me.es.osaka-u.ac.jp

In the confocal microscopy, sub-micron resolution is achieved in the depth direction. For example, the depth resolution becomes $\sim$ 250 nm from the theoretical formula,[25] when the numerical aperture of an objective lens is 1.4 and wavelength of the pump light is 400 nm. The confocal optics is obtained by adding pinholes and lenses in optics, and it can be combined with setup of several optical measurements; the confocal optics has been combined with Raman spectroscopy[26] and Brillouin microscopy[27] for evaluating local properties. Because picosecond ultrasonics is also an optical technique, we have considered that by combining the confocal optics with optics of the picosecond ultrasonics, propagation of acoustic waves will be visualized, and a feasibility study was performed.[28] In this brief note, we describe the detail of the confocal optics developed for picosecond ultrasonics. Using the optics, we observe that a waveform measured in the experiment changes from a damped oscillation to a wave packet and it moves when the focal point of the objective lens is moved in the depth direction of a specimen, visualizing the propagation of the acoustic wave.

In picosecond ultrasonics, acoustic waves are excited and detected using the pump-probe method. Specimen surface is irradiated with ultrashort (picosecond or femtosecond) pulse laser, so-called pump light, and acoustic waves are exited through instantaneous thermal expansion near the specimen surface. Longitudinal acoustic pulse then propagates in the thickness direction in the specimen. The specimen surface is irradiated with another pulse laser, so-called probe light, after the acoustic waves are excited. A part of the probe light transmits into the specimen, and it is backscattered by the acoustic pulse. The backscattered light and the probe light reflected at the specimen surface are detected by the detector. When delay time of the probe light is changed, intensity of the detected light changes oscillatory, because length of the optical path of the backscattered light changes as the acoustic wave propagates, and constructive and destructive interferences occur. This phenomenon is called Brillouin oscillation, and frequency f_B of the oscillation is expressed as $f_B = 2nv/\lambda$, where n is the refractive index of the specimen, v the sound velocity of longitudinal wave, and λ the wavelength of the probe light.[1] Therefore, sound velocity and elastic stiffness of transparent materials can be determined by measuring f_B.

In the present study, a confocal optics is embedded in the optics for the Brillouin-oscillation measurement. Figure 1(a) shows the optics of the backscattered probe light in the conventional picosecond ultrasonics. When acoustic pulse arrives at the focal point at $t = t_0$, the probe light is scattered by the acoustic pulse, and it is detected by the detector. When the acoustic pulse propagates further ($t = t_0 + \Delta t$), it is not located at the focal point. However, a part of the probe light is backscattered and it is detected by the detector as well.

Then, amplitude and/or phase of detected light shows an oscillation pattern as shown in Fig. 1(c). Frequency of the oscillation is determined by applying the fast Fourier transformation (FFT) to it, and sound velocity is determined from the frequency. The sound velocity is the value averaged over the path where the acoustic pulse propagates.

In the optics of confocal picosecond ultrasonics, a pinhole and lenses are inserted as shown in Fig. 1(b). When the probe light is backscattered by the acoustic pulse at the focal plane ($t = t_0$), the light passes through the pinhole, and it is detected by the detector. However, when the acoustic wave propagates further ($t = t_0 + \Delta t$), the pinhole shields the probe light, and intensity of the probe light becomes significantly small. In principle, light reflected at the specimen surface cannot pass through the pinhole either. However, intensity of the reflected light is stronger than that of the backscattered light, and it is difficult to shield the reflected light completely using the pinhole. Then, the detected signal will show a wave packet as shown in Fig. 1(c). The wave packet should shift by changing the position of the focal point. Therefore, by measuring the shift of the wave packet with moving the focal point, propagation of the acoustic wave is visualized and local sound velocity will be determined.

Both the confocal picosecond ultrasonics and the wavelet transforms using the conventional picosecond ultrasonics show sub-micron resolution in the thickness direction. However, the confocal picosecond ultrasonics shows better acoustic-wave selectability than the wavelet transforms. For example, when an acoustic pulse propagating in a thin film deposited on substrate arrives at the interface between the film and substrate, reflected and transmitted acoustic pulses are generated. Using the conventional picosecond ultrasonics, both pulses are detected. When frequency of the Brillouin oscillation for reflected pulse is close to that for the transmitted pulse, it becomes difficult to distinguish them using the wavelet transforms. In contrast, in the picosecond ultrasonics, an acoustic pulse that arrives at the focal point is detected. Therefore, by moving the focal point, reflected and transmitted waves can be detected individually.

Figure 2 shows the optics that was developed in the present study, in which some optical elements such as filters and collimators are not shown for simplicity. Two femtosecond lasers were used as the light sources. The lasers are synchronized. Wavelength of the lights was 800 nm, and the repetition rate was 80 MHz. The pump light was modulated at 1 MHz for lock-in detection by passing through the acousto-optic modulator (AOM). Primary diffracted light was reflected at a dichroic mirror (DM). The probe beam passed through the second-harmonic-generation (SHG) crystal to generate second-harmonic light with the center wavelength of 400 nm. A part of the light was reflected by a beam sampler to be used for the

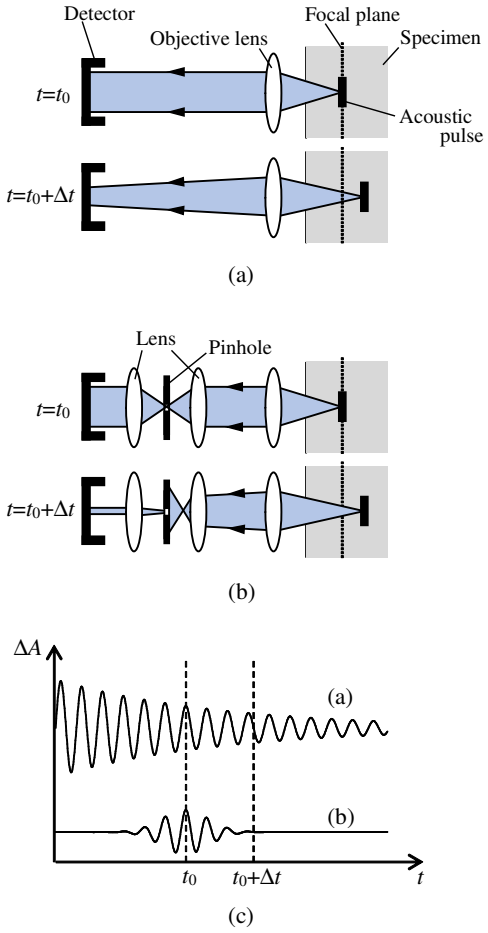

Fig. 1. Schematics of optical path of probe light scattered by acoustic pulse for (a) conventional picosecond ultrasonics and (b) confocal picosecond ultrasonics. At $t = t_0$, an acoustic pulse arrives at the focal plane, and it is out of the focal plane at $t = t_0 + \Delta t$. (c) Expected signals obtained by (a) conventional and (b) confocal picosecond ultrasonics.

reference light of the balanced detector. The light passing through the beam sampler passes through the DM with the same light axis as that of the pump light. The pump and probe light are introduced into the confocal laser scanning microscope (Nikon, A1R). The lights are reflected by the beam splitter, and irradiate the specimen surface through an objective lens. Reflected lights are then pass through the pinhole, and the probe light is detected by the balanced detector. By moving the corner reflector, delay time of the probe light was changed with sub-picosecond time resolution. The magnification of the objective lens was 40, and its numerical aperture was 0.95. Power of the pump light was 3 mW, and that of the probe light was 16 mW. Size of the pinhole was controlled by the software equipped with the microscope.

Specimen was silica film deposited on a quartz substrate by RF magnetron sputtering.

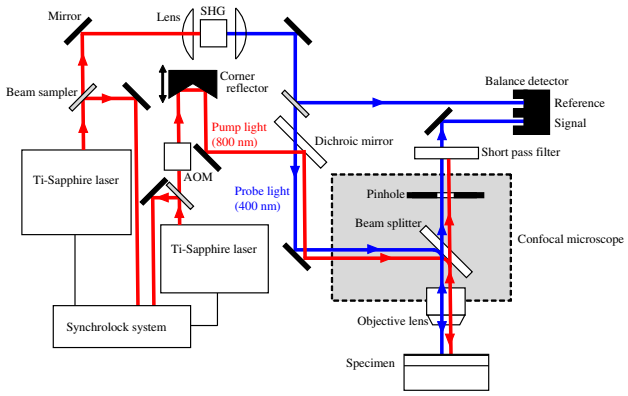

Fig. 2. Optics developed for confocal picosecond ultrasonics.

Film thickness was $\sim 2\ \mu$m. Aluminum film with thickness of ~ 10 nm was deposited on the film surface as a sound source.

First, the picosecond ultrasonics measurement was performed with maximum pinhole diameter (focal depth displayed in the software was 11 μm). The result is shown in Fig. 3(a). The intensity increases rapidly at 0 ps, indicating that an acoustic pulse was excited around this time. Then, damped oscillation of the intensity was observed, which is a typical waveform of the Brillouin oscillation. Frequency of the Brillouin oscillation was deduced using FFT. Gate width of FFT was 50 ps, and frequency was calculated with moving the gate position as shown in Fig. 3(b). When the gate includes the data above 333 ps, notable change in the frequency was observed, indicating that the acoustic wave arrived at the interface between the silica film and quartz substrate. Therefore, frequency of Brillouin oscillation of the silica glass film was calculated from the data in 0-283 ps, and it was 40.4 GHz. Using refractive index of vitreous SiO_2, $n = 1.47$,[9] the sound velocity of acoustic pulse was calculated to be 5497 m/s.

Then, size of the pinhole was decreased so that the focal depth becomes 1 μm, and the picosecond ultrasound measurement was performed. Figure 3(c) shows the results. The waveform is different from that observed in Fig. 3(a), and a wave packet is observed clearly. The wave packet moved when the objective lens was moved in the depth direction. The dashed line in Fig. 3(c) represents the peak position of the wave packet estimated from the sound velocity obtained from the Brillouin oscillation above. Apparently, position of the measured wave packet shows agreement with the dashed line, indicating that propagation of the acoustic pulse is visualized and the confocal optics is well established for the picosecond ultrasonics. In the present setup, refraction of the probe light at interface between air and the specimen

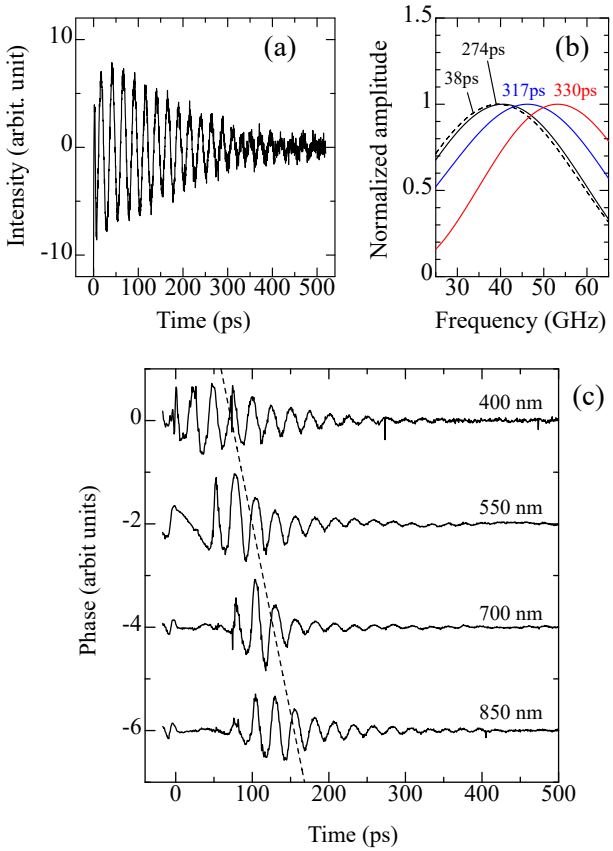

Fig. 3. (a) Signal obtained for silica film deposited on quartz with the pinhole full open, and (b) its Fourier spectra with different gate positions. Gate width is 50 ps, and the center position of the gate are described. (c) Signals obtained by the confocal picosecond ultrasonics by moving the objective lens in the depth direction. Distance from the film surface to the focal point is changed from 400 to 850 nm. For comparison, shift of the peak position calculated from the sound velocity (5497 m/s) is plotted by the dashed line. The waveforms in (a) and at 700 nm in (c) were reported in our previous work.[28)]

surface occurs. Then, the shift of the focal point becomes smaller than that of the objective lens depending on the refractive index of the specimen and incident angle of the probe light. In the above comparison between position of the measured wave packet and estimated position, this effect is not considered. Consideration of this effect will be required for evaluating the sound velocity precisely.

In this study, we developed the optics for confocal picosecond ultrasonics. A wave packet was observed clearly in the silica film, and shift of the wave packet was observed, when the objective lens (focal point) was moved. This method will allow us to evaluate local sound velocity of micro/nano-meter transparent materials.

This research was supported by the Innovative Project for Advanced Instruments, Renovation Center of Instruments for Science Education and Technology, Osaka University.

References

1) C. Thomsen, H. T. Grahn, H. J. Maris, and J. Tauc, Phys. Rev. B **34**, 4129 (1986).
2) B. M. Clemens and G. L. Eesley, Phys. Rev. Lett. **61**, 2356 (1988).
3) E. E. Fullerton, I. K. Schuller, F. T. Parker, K. A. Svinarich, G. L. Eesley, R. Bhadra, and M. Grimsditch, J. Appl. Phys. **73**, 7370 (1993).
4) B. Perrin, B. Bonello, J.-C. Jeannet, and E. Romater, Physica B **219&220**, 681 (1996).
5) N. Nakamura, H. Ogi, T. Yasui, M. Fujii, and M. Hirao, Phys. Rev. Lett. **99**, 035502 (2007).
6) N. Nakamura, R. Yokomura, N. Takeuchi, D. Yamakado, and H. Ogi, Jpn. J. Appl. Phys. **58**, 075504 (2019).
7) T. C. Zhu, H. J. Maris, and J. Tauc, Phys. Rev. B **44**, 4281 (1991).
8) A. Devos, M. Foret, S. Ayrinhac, P. Emery, and B. Rufflê, Phys. Rev. B **77**, 100201 (2008).
9) H. Ogi, T. Shagawa, N. Nakamura, M. Hirao, H. Odaka, and N. Kihara, Phys. Rev. B **78**, 134204 (2008).
10) P. Babilotte, P. Ruello, G. Vaudel, T. Pezeril, D. Mounier, J.-M. Breteau, and V. Gusev, Appl. Phys. Lett. **97**, 174103 (2010).
11) A. Nagakubo, M. Arita, T. Yokoyama, S. Matsuda, M. Ueda, H. Ogi, and M. Hirao, Jpn. J. Appl. Phys. **54**, 07HD01 (2015).
12) H Ogi, M. Fujii, N. Nakamura, T. Yasui, and M. Hirao, Phys. Rev. Lett. **98**, 195503 (2007).
13) N. Nakamura, H. Ogi, and M. Hirao, Phys. Rev. B **77**, 245416 (2008).
14) N. Nakamura, A. Uranishi, M. Wakita, H. Ogi, M. Hirao, and M. Nishiyama, Appl. Phys. Lett. **98**, 101911 (2011).
15) C. Rossignol, N. Chigarev, M. Ducousso, B. Audoin, G. Forget, F. Guillemot, and M. C. Durrieu, Appl. Phys. Lett. **93**, 123901 (2008).
16) T. Dehoux and B. Audoin, J. Appl. Phys. **112**, 124702 (2012).
17) S. Danworaphong, M. Tomoda, Y. Matsumoto, O. Matsuda, T. Ohashi, H. Watanabe, M. Nagayama, K. Gohara, P. H. Otsuka, and O. B. Wright, Appl. Phys. Lett. **106**, 163701 (2015).
18) G. Hall, Ultrasonics **15**, 57 (1977).
19) K. Sato, R. Shintate, M. Fujiwara, and Y. Saijo, Jpn. J. Appl. Phys. **58**, SGGE19 (2019).
20) Y. Ohara, J. Potter, H. Nakajima, T. Tsuji, and T. Mihara, Jpn. J. Appl. Phys. **58**,

SGGB06 (2019).

21) M. Minsky, Scanning **10**, 128 (1988).

22) G. J. Brakenhoff, H. T. M. van der Voort, E. A. van Spronsen, W. A. M. Linnemans, and N. Nanninga, Nature **317** 748 (1985).

23) A. Gruber, A. Dräbenstedt, C. Tietz, L. Fleury, J. Wrachtrup, and C. von Borczyskowski, Science **276**, 2012 (1997).

24) N. Nakamura, S. Nakashima, and H. Ogi, Sci. Rep. **9**, 12836 (2019).

25) R. W. Cole, T. Jinadasa, and C. M. Brown, Nat. Protoc. **6**, 1929 (2011).

26) G. J. Puppels, F. F. M. de Mul, C. Otto, J. Greve, M. Robert-Nicoud, D. J. Arndt-Jovin, and T. M. Jovin, Nature **347**, 301 (1990).

27) G. Scarcelli and S. H. Yun, Nat. Photonics **2**, 39 (2008).

28) N. Nakamura, A. Maehara, and H. Ogi, Proc. Symp. Ultrason. Electron. **40**, 2E1-3 (2019).